Determining metabolic mechanism linking phospholipids and docosahexaenoic acid through phosphatidylcholine synthesis by *phosphocholine cytidylyltransferase (CCT)* overexpression in *Schizochytrium* sp

Xiaowen Cui[1,2], Tingting Chen[1], Yizhen Meng[1], Xueshan Pan[3], Ruizhe Wu[1], Yinghua Lu[1,2*], Chuanyi Yao[1,2], Xihuang Lin[4] and Xueping Ling[1,2*]

Abstract

The polyunsaturated fatty acid (PUFA) metabolism of *Schizochytrium*, an excellent oil-producing microorganism, is closely related to phosphatidylcholine (PC) synthesis, which favors the migration and accumulation of docosahexaenoic acid (DHA). Phosphocholine cytidylyltransferase (CCT), a key enzyme involved in PC synthesis, profoundly impacts lipid metabolism in plants; however, few studies have focused on CCT in microorganisms. We investigated the effects of *CCT* overexpression on lipid metabolism in *Schizochytrium* sp. *CCT* overexpression slightly inhibited cell growth, but significantly promoted total lipid synthesis. Compared to the wild-type strain, PUFA content and DHA production in the CCT-overexpressing strain (SR21-CCT) increased by about 49% and 46%, respectively. Analysis of phospholipids and quantitative real-time PCR revealed that *CCT* overexpression enhanced phospholipid synthesis, especially by strengthening glycerophosphorylcholine acylation and *de novo* PC synthesis pathways, which promote DHA esterification to PC and DHA accumulation in triacylglycerols. This study helps decipher the mechanism correlating phospholipid metabolism and DHA production.

Keywords Phosphocholine cytidylyltransferase, Docosahexaenoic acid, Phosphatidylcholine pathway, Phospholipid synthesis

*Correspondence:
Yinghua Lu
ylu@xmu.edu.cn
Xueping Ling
xpling@xmu.edu.cn
[1]Department of Chemical and Biochemical Engineering, College of Chemistry and Chemical Engineering, Xiamen University, Xiamen, P.R. China
[2]Xiamen Key Laboratory of Synthetic Biotechnology, Xiamen University, Xiamen, P.R. China
[3]Department of Biochemistry and Molecular Biology, School of Laboratory Medicine, Bengbu Medical University, Bengbu, P.R. China
[4]Analysis and Test Center, Third Institute of Oceanography, Ministry of Natural Resources, Xiamen, P. R. China

Introduction

Schizochytrium sp. is a marine protist that synthesizes various beneficial active substances, such as PUFAs [1, 2], squalene [3, 4], and pigments [5]. As the most abundant type of PUFA in *Schizochytrium*, the mechanism of docosahexaenoic acid (DHA) biosynthesis has been extensively explored. Three main forms of DHA have been reported in cells: non-esterified fatty acid DHA (DHA-FFA), triacylglycerol (TAG) DHA (DHA-TAG), and phospholipids (PLs) DHA (DHA-PLs) [6]. Recent studies have revealed that DHA is mainly biosynthesized through the anaerobic polyketide synthase (PKS) pathway, released as DHA-FFA, incorporated into polar PLs such as phosphatidylcholine (PC), phosphatidylethanolamine (PE), and phosphatidylinositol (PI) to form DHA-PLs, and finally transferred from DHA-PLs to non-polar lipids such as TAG to form DHA-TAG for storage via the acyl-CoA-independent pathway [7–10]. Therefore, regulating PL metabolism plays a significant role in DHA accumulation. By improving the phosphatidic acid (PA) synthesis pathway in *Aurantiochytrium limacinum* F26-b, more DHA is bound into glycerol-3-phosphate (G3P), thus significantly increasing the DHA content in PC and TAG [11]. PC is the main PL that esterified with DHA in *Schizochytrium* [12]. Hence, modifying the PC metabolic pathway is feasible and effective strategy to regulate DHA synthesis and accumulation.

PC is primarily synthesized via three pathways, as shown in Fig. 1. The first is the *de novo* synthetic pathway [13], which starts with choline and produces phosphocholine (P-Cho) through the catalysis of choline kinase (CK), then P-Cho and cytidine-5′-triphosphate are condensed to form cytidine diphosphocholine (CDP-Cho) by phosphocholine cytidyltransferase (CCT). Subsequently, the P-Cho group is transferred onto diacylglycerol (DAG) to produce PC, which is catalyzed by choline phosphotransferase (CPT) [14]. The second pathway is called the glycerophosphorylcholine (GPC) acylation pathway, in which the glycerol-3-phosphate choline substrate is catalyzed by glycerophosphocholine acyltransferase (GPCAT) and lysophosphatidylcholine acyltransferase (LPCAT) for the subsequent synthesis of PC [14, 15]. The third pathway involves the synthesis of PC from PE via transmethylation [16]. According to lipidomic analyses of *Schizochytrium*, PLs have a very low PE content, which only accounts for about 3–10%, whereas the PC content is approximately 40–50% [12, 17]. Therefore, it was inferred that PC synthesis from PE is not the main pathway. GPCAT and LPCAT from the GPC acylation pathway have rarely been reported in PC synthesis,

Fig. 1 The synthesis pathways of PC. (**Cho**, choline; **P-Cho**, phosphocholine; **CDP-Cho**, cytidine diphosphocholine; **PC**, phosphatidylcholine; **CK**, choline kinase; **CCT**, phosphocholine cytidyltransferase; **CPT**, choline phosphotransferase; **Etn**, ethanolamine; **P-Etn**, phosphoethanolamine; **CDP-Etn**, cytidine diphosphoethanolamine; **PE**, phosphatidylethanolamine; **EK**, ethanolamine kinase; **ECT**, ethanolamine phosphate cytidylyltransferase; **EPT**, ethanolamine phosphotransferase; **TAG**, triacylglycerol; **DAG**, diacylglycerol; **PEMT**, phosphatidylethanolamine *N*-methyltransferase; **PDAT**, phospholipid: DAG acyltransferase; **PDCT**, PC: DAG cholinephosphotransferase; **DGAT**, phospholipid: DAG acyltransferase; **G3PC**, Glycero-3-phosphocholine; **LPC**, lysophosphatidylcholine; **GPCAT**, glycerophosphorylcholine acyltransferase; **LPCAT**, lysophosphatidylcholine acyltransferase)

whereas CCT is reportedly the rate-limiter in PC synthesis [18–20], which may contribute to the homeostasis of PL composition. Currently, research on CCT is limited and mainly focuses on animal organs and insects, with few studies on microorganisms.

This study aimed to investigate the effect of PC biosynthesis regulation on the production of lipids and DHA by overexpressing the *CCT* gene in *Schizochytrium limacinum* SR21 (*S. limacinum* SR21). To further explore the regulatory mechanism of PC synthesis on DHA accumulation, PL lipidomics and quantitative real-time PCR (qRT-PCR) were used to analyze changes in metabolites and gene expression, which would further bolster evidence of the correlation between PL metabolism and DHA accumulation in *Schizochytrium* sp.

Materials and methods

Strains and culture conditions

S. limacinum SR21 (ATCC MYA-1381) was obtained from the American Type Culture Collection (Manassas, VA, USA) and was cultured in the seed medium [30 g/L glucose, 10 g/L yeast extract, 50 mL 500× inorganic salt solution (Na_2SO_4 240 g/L, $MgSO_4$ 40 g/L, KH_2PO_4 20 g/L, $(NH_4)_2SO_4$ 20 g/L, K_2SO4 13 g/L, KCl 10 g/L) and 0.17 g/L $CaCl_2$] at 28 °C and 200 rpm in flasks. After two generations of cultivation, the seed cultures were transferred to the fermentation medium reported in our previous study and cultivated at 28 °C and 200 rpm for 144 h.

Overexpression of *CCT*

The primers, plasmids, and strains used in this study are listed in Supplementary file (Table S1). The plasmid pBlu-zeo-18s, containing homologous arms from 18s rRNA and *zeo^r* for screening, was constructed in our previous study [21]. The *CCT* (GenBank: PQ289629) fragment was amplified with CCT-F/CCT-R from *S. limacinum* SR21 genome and ligated into pBlu-zeo-18s at the corresponding restriction enzyme cutting sites, resulting in the recombinant plasmid pBlu-zeo-18s-*CCT*. The recombinant plasmid was electroporated into *S. limacinum* SR21 with conditions set at 2 kV, 50 µF and 200 Ω, and the electroporated cells were resuscitated in the seed medium containing 1 M sorbitol (Macklin Biochemical, Shanghai, China) for 3 h at 28 °C and then recovered for 3–5 d in a solid medium containing 50 µg/mL zeocin (Sangon Biotech, Shanghai, China) for screening the positive mutant strains.

Biomass determination, lipid extraction, and separation

The cell pellets were obtained by centrifuging at 8000 rpm for 5 min, washed twice with phosphate buffered saline, and freeze-dried to a constant weight, which was determined as the dry cell weight (DCW) of the biomass.

The cell pellets from 5 mL fermentation liquid were resuspended with 37% HCl and saponified at 65 °C water bath for 1 h. Total lipids (TLs) were extracted using 15 mL of n-hexane and weighed after nitrogen blowing. Solid-phase extraction (SPE, Shanghai Jinlan, China) was used to analyze the proportion of fatty acids in polar and non-polar lipids. Twenty-five milligrams of TLs were dissolved in 1 mL of trichloromethane/methanol solution (2:1, v/v) with the addition of 20 µL PC (19:0/19:0) as the internal standard, and then they were added to SPE activated with n-hexane. Non-polar lipids were first obtained by sequentially elution with 4 mL of n-hexane/ether solution in two volume ratios (4:1 and 1:1, v/v). Polar lipids were eluted using 5 mL methanol and 6 mL chloroform/methanol/aqueous solution (3:5:2, v/v/v).

Thin-layer chromatography (TLC) and gas chromatography (GC) analysis

TLC could confirm the lipid profiles in polar lipids and non-polar lipids, the corresponding developing solvent systems of which were chloroform/methanol/acetic acid/water of 90:15:10:3 (v/v) and hexane/diethyl ether/acetic acid of 70:30:1(v/v), respectively. TAG-18:1/18:1/18:1, FFA-22:5, and DAG-18:1/18:1 was used as standards to confirm the presence of TAG, FFA, and DAG bands in the samples. For better observation, TLC silica gels were placed in a closed container for 10 min along with solid iodine and bands were observed.

To obtain the sample of fatty acid methyl ester (FAMEs), 5 mL of 0.1 M $KOH-CH_3OH$ was first added into the TLs in 65 °C water bath for 5 min and cooled to 28 °C. Then, 5 mL of boron trifluoride ether was added to catalyze the methyl ester reaction in a 65 °C water bath for 30 min. Finally, 5 mL of n-hexane was added to extract the FAMEs, and 1 mL of saturated NaCl solution was added to prevent emulsification. FAMEs were analyzed using a Shimadzu GC-2010 instrument (Shimadzu, Japan) equipped with an HP-88 (100 m × 0.25 mm ID, 0.20 µm film) capillary column using nitrogen as the carrier gas at a constant flow rate of 0.6 mL/min. The GC temperature programming was increased from 140 °C to 210 °C at increments of 4 °C/min and held for 31.5 min, and then heated to 230 °C at a rate of 10 °C/min and maintained for 3 min. Finally, the temperature reached 240 °C at an increment of 10 °C/min and held for 10 min. The temperature of injection and flame ionization detector were 260 °C. The peak time of each sample component was determined according to a mixed standard containing 37 FAMEs (CRM47885, Sigma-Aldrich, Germany).

Quantification of PLs

The obtained polar lipids by SPE were analyzed using ultra performance liquid chromatography-mass

spectrometry (Waters UPLC Acquity H-Class-Xevo-G2 Q-TOF, Milford, MA, USA) equipped with a Waters UPLC BEH C18 column (150 mm ×2.1 mm × 1.7 μm). The binary mobile phase solvent system consisted of A (acetonitrile) and B (20 mM ammonium formate buffer by adding 0.1% formic acid to obtain a pH 3.5). The separation was processed in a gradient elution as follows: 0–4 min, 95% A;4–22 min, 95–60% A; 22–25 min, 60% A; 25–25.1 min, 60–95% A; 25.1–30 min, 95% A. The injection volume was 2 μL and the flow rate was 0.2 mL/min. The experimental parameters were set as follows: sensitivity mode; data collection time: 2.5–20 min; scanning range: 250–1000 Da; scanning time 0.5 s; capillary voltage 2 kV; sample cone voltage 30 V; extraction cone voltage 4 V; ion source temperature: 100 °C; desolvation temperature: 350 °C; cone gas flow rate 50 L/h; desolvation gas flow rate 400 L/h.

Quantitative real-time PCR analysis (qRT-PCR)

Total RNA was extracted from 1 mL of fresh fermentation solution using a *Steady Pure* Universal RNA Extraction Kit II (Accurate Biotechnology, China). Both the reverse transcription of total RNA and the qRT-PCR of cDNA were performed using the *PerfectStart*® Uni RT&qPCR Kit (TransGen Biotech, China) according to the manufacturer's instructions. The primers used for qRT-PCR are listed in Table S1. The reference gene was *actin.* The relative transcription level was represented by $2^{-\Delta\Delta CT}$ values.

Calculation and statistical analysis

All experiments were performed in triplicate. Statistical significance was evaluated using a *t*-test ($p < 0.01$, extremely significant; $0.01 < p < 0.05$, statistically significant). Data are presented as means ± standard deviation.

Results

Construction of *CCT*-overexpressing strain

The *CCT* gene was amplified by PCR using *S. limacinum* SR21 genomic DNA as a template with a length of approximately 1840 bp (Fig. S1). The plasmid pBlu-zeo-18s-CCT was successfully constructed (Fig. S2A), and a mutant strain was successfully transformed (Fig. S2B).

Changes of biomass, TLs and DHA production

As shown in Fig. 2A, the wild-type strain (SR21) showed a growing advantage in the early fermentation period compared with the mutant strain overexpressing *CCT* (SR21-CCT) and reached the highest biomass of 37.8 g/L when entering the stationary phase at 72 h. Overexpression of *CCT* led to delayed cell growth, leading to SR21-CCT entering the stationary phase after 96 h and achieving a similar maximum biomass as SR21. Among the changes in total oil, the time to reach the peak

of SR21 was 96 h, while the mutant strain was 120 h. Although lipid synthesis of SR21-CCT was also delayed 24 h to reach its highest value compared to that of SR21, the TLs yield of SR21-CCT increased by 20.6% than that of SR21. Notably, both the DHA titer and DHA productivity of SR21-CCT remained higher than those of SR21 through the process, the highest values of which in SR21-CCT obtained at 120 h were increased by 75.8% and 83.7% compared with that of SR21 at 96 h, respectively, reaching 10.7 g/L and 0.3 g/g DCW (Fig. 2B). The highest TLs content of SR21-CCT was also reached at 120 h, which was 28.4% higher than the highest TLs (96 h) of SR21 (Fig. 2C).
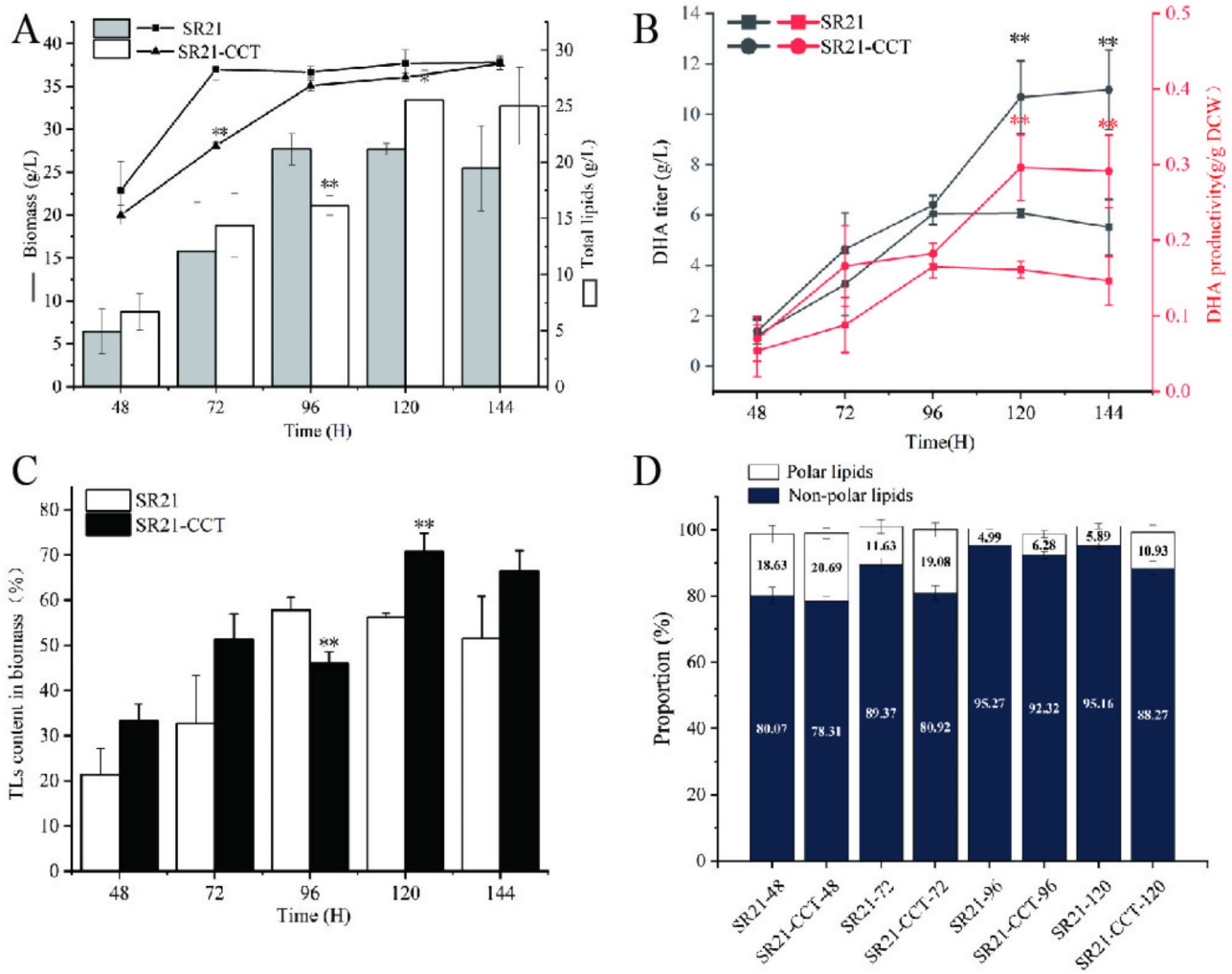
Changes of lipids profile

Figure 2D shows that the content of non-polar lipids gradually increased with cell growth and lipid accumulation and reached a peak at 96 h in both strains. Conversely, the content of polar lipids in both strains accounted for the highest proportion in the early stage of lipid synthesis (48 h) and gradually decreased with time, reaching the lowest value at 96 h. Compared with the wild-type strain, the overexpression of *CCT* increased the proportion of polar lipids during the whole cell growth, which increased by 11.1%, 64.1%, 25.9%, and 85.6% at the early stage (48 h), middle stage (72 h), and late stages (96 h and 120 h) of lipid synthesis, respectively.

As shown in Fig. S3, TAG are the main components of non-polar lipids throughout the fermentation process. Compared to SR21, the TAG content in SR21-CCT showed an obvious increase at 48 h and hardly changed from 96 to 120 h. The other two components of non-polar lipids were FFA and DAG.

Changes of fatty acids composition in TLs, non-polar lipids and Polar lipids

Overall, *CCT* overexpression significantly reduced the saturated fatty acid (SFA) proportion and correspondingly increased the PUFAs proportion (Table 1), which resulted in the ratio of PUFAs/SFAs content in SR21-CCT increased by 120.6% at 120 h than that in SR21. At 120 h, the proportion of SFAs in SR21-CCT strain reduced by 32.1%, while the proportions of PUFAs and DHA increased by 48.9% and 45.6%, respectively, compared with those in the wild-type strain. In particular, the reduction in SFAs was mainly reflected in the decrease in C16:0, which decreased by 33.6% at 120 h. Interestingly, the PUFAs or DHA contents in the mutant strain were lower than those in the wild-type strain at the early stage of fermentation (48 h), but higher than that in the wild-type strain at the middle and late stages of fermentation (72–120 h).

As listed in Table 2, for fatty acids of non-polar lipids, C16:0 is the main component of the SFAs while DHA/

Fig. 2 The fermentation result of SR21 and SR21-CCT strains. (**A**) biomass (line) and TLs yield (bar), (**B**) DHA titer and productivity, (**C**) the TLs content in biomass, and (**D**) the lipid profiles, in SR21 and SR21-CCT strains during the fermentation process. Note: *p-value < 0.05 and **p-value < 0.01, compared to SR21 at each time

Table 1 The main fatty acids proportion of total lipids in SR21 and SR21-CCT strain at different stages of fermentation

Fatty acid	SR21				SR21-CCT			
	48 h	72 h	96 h	120 h	48 h	72 h	96 h	120 h
C14:0	2.43±0.48%	3.30±0.01%	3.34±0.06%	3.28±0.05%	1.46±0.60%	1.69±0.11%**	1.96±0.02%**	1.93±0.13%**
C16:0	42.3±6.73%	50.9±0.09%	50.2±0.28%	49.6±0.23%	27.3±9.17%*	31.6±1.68%**	33.9±0.09%**	32.9±1.05%**
C18:0	2.04±0.06%	1.55±0.04%	1.61±0.16%	1.62±0.11%	2.89±0.58%	1.45±0.29%	1.30±0.04%*	1.21±0.15%
EPA	0.10±0.02%	0.14±0.00%	0.31±0.01%	0.35±0.00%	0.03±0.05%	0.08±0.01%	0.11±0.01%**	0.12±0.01%**
DPA	4.82±0.30%	5.09±0.11%	5.52±0.07%	5.64±0.03%	4.21±0.21%	6.99±0.87%*	9.36±0.06%**	10.1±0.16%**
DHA	25.1±2.06%	26.9±0.48%	28.6±0.16%	28.7±0.03%	20.8±2.50%	32.4±3.58%	39.6±0.22%**	41.8±1.23%**
SFAs	49.4±7.05%	58.2±0.39%	56.8±0.54%	56.1±0.40%	35.8±9.79%*	36.7±1.82%**	39.1±0.05%**	38.1±1.47%**
PUFAs	31.1±2.20%	32.8±0.61%	35.1±0.23%	35.4±0.03%	26.4±2.74%	40.3±4.37%	49.7±0.30%*	52.7±1.56%*
PUFAs/SFAs	0.63±0.13	0.56±0.01	0.62±0.01	0.63±0.01	0.74±0.28	1.10±0.17**	1.27±0.01**	1.39±0.09**

Note: *p-value < 0.05 and **p-value < 0.01, compared to SR21 at each time

DPA are that of PUFAs. Generally, the fatty acid composition of the non-polar lipids in SR21-CCT displayed a similar change to that in the TLs of SR21-CCT (Table 1); that is, the *CCT* overexpression drastically reduced the content of SFAs and enhanced the content of PUFAs in the non-polar lipids of SR21-CCT. For both strains, the proportion of DHA in non-polar lipids continuously increased throughout the fermentation process.

Table 2 The main fatty acids composition of non-polar lipid in SR21 and SR21-CCT strain during the fermentation

Fatty acid	SR21				SR21-CCT			
	48 h	72 h	96 h	120 h	48 h	72 h	96 h	120 h
C14:0	2.63 ± 0.75%	3.69 ± 0.44%	3.46 ± 0.03%	3.30 ± 0.38%	1.91 ± 0.09%	2.07 ± 0.29%	2.91 ± 0.15%**	2.61 ± 0.03%**
C16:0	42.1 ± 0.59%	53.9 ± 1.35%	51.4 ± 0.75%	51.0 ± 0.85%	29.5 ± 0.50%**	31.6 ± 0.77%**	32.8 ± 0.49%**	32.2 ± 0.39%**
C18:0	0.55 ± 0.57%	1.15 ± 0.06%	1.24 ± 0.08%	1.08 ± 0.06%	0.92 ± 0.26%	0.37 ± 0.08%**	0.77 ± 0.04%**	0.45 ± 0.03%**
EPA	0.12 ± 0.01%	0.15 ± 0.05%	0.33 ± 0.01%	0.33 ± 0.04%	0.04 ± 0.02%**	0.07 ± 0.01%*	0.11 ± 0.02%**	0.12 ± 0.02%**
DPA	4.86 ± 0.24%	4.97 ± 0.06%	5.01 ± 0.17%	5.53 ± 0.22%	4.24 ± 0.13%	7.06 ± 0.16%**	9.86 ± 0.12%**	10.8 ± 0.17%**
DHA	26.2 ± 1.15%	26.4 ± 0.34%	29.9 ± 0.22%	29.1 ± 1.35%	22.5 ± 0.20%*	33.4 ± 0.52%**	40.7 ± 0.08%**	44.1 ± 0.55%**
SFAs	47.3 ± 0.84%	60.7 ± 0.98%	58.1 ± 0.75%	57.4 ± 0.59%	34.3 ± 0.42%**	36.1 ± 0.46%**	38.5 ± 0.62%**	37.3 ± 0.36%**
PUFAs	31.1 ± 1.01%	31.5 ± 0.70%	35.3 ± 0.18%	35.0 ± 1.56%	26.8 ± 0.25%*	40.5 ± 0.42%**	50.7 ± 0.04%**	55.0 ± 0.71%**
PUFAs/SFAs	0.66 ± 0.03	0.52 ± 0.02	0.61 ± 0.01	0.61 ± 0.03	0.78 ± 0.02*	1.12 ± 0.03**	1.32 ± 0.02**	1.47 ± 0.03**

Note: *p-value < 0.05 and **p-value < 0.01, compared to SR21 at each time

Table 3 The fatty acids composition of the Polar lipids in SR21 and SR21-CCT strains during the fermentation

Fatty acid	SR21				SR21-CCT			
	48 h	72 h	96 h	120 h	48 h	72 h	96 h	120 h
C14:0	1.17 ± 0.09%	0.66 ± 0.12%	0.75 ± 0.30%	0.89 ± 0.33%	0.36 ± 0.01%**	0.48 ± 0.28%	0.31 ± 0.04%	0.45 ± 0.16%
C16:0	31.5 ± 0.94%	24.4 ± 1.71%	24.3 ± 1.35%	26.3 ± 1.14%	23.2 ± 0.31%**	22.8 ± 1.16%	22.4 ± 1.22%	21.8 ± 1.48%**
C18:0	8.41 ± 1.56%	5.33 ± 0.22%	7.25 ± 1.42%	8.70 ± 0.24%	9.64 ± 0.33%	5.90 ± 0.74%	9.09 ± 0.64%	7.53 ± 0.99%
EPA	0.07 ± 0.05%	0.05 ± 0.03%	0.20 ± 0.03%	0.19 ± 0.09%	0%	0.15 ± 0.04%	0.20 ± 0.02%	0.23 ± 0.08%
DPA	4.18 ± 0.15%	5.27 ± 0.72%	3.80 ± 0.48%	4.18 ± 0.42%	4.79 ± 0.69%	5.01 ± 0.54%	4.17 ± 0.84%	4.81 ± 0.91%
DHA	17.7 ± 2.77%	30.0 ± 0.87%	17.6 ± 1.48%	15.4 ± 0.34%	14.9 ± 0.68%	26.7 ± 0.47%**	24.0 ± 0.75%**	23.5 ± 3.97%**
SFAs	44.8 ± 3.04%	33.0 ± 2.21%	34.8 ± 0.36%	39.7 ± 0.93%	40.0 ± 0.97%	32.7 ± 1.95%	34.7 ± 1.03%	32.4 ± 1.50%**
PUFAs	24.6 ± 2.01%	37.3 ± 0.49%	23.6 ± 1.76%	21.5 ± 0.32%	25.7 ± 0.55%	34.9 ± 0.89%*	33.6 ± 0.96%**	31.5 ± 3.83%**
PUFAs/SFAs	0.55 ± 0.08	1.13 ± 0.09	0.68 ± 0.06	0.54 ± 0.02	0.64 ± 0.03	1.07 ± 0.09	0.97 ± 0.06**	0.97 ± 0.16**

Note: *p-value < 0.05 and **p-value < 0.01, compared to SR21 at each time

Moreover, the proportion of DHA in SR21-CCT at 48 h was lower than that in the wild-type strain, but higher than that in the wild-type strain from 72 to 120 h, which was consistent with the change in the TLs. Compared with that in the wild-type strain at 120 h, SFA proportion of non-polar lipids in SR21-CCT reduced by 35.0%, and PUFAs and DHA proportion of non-polar lipids in SR21-CCT increased by 57.1% and 51.5%, respectively.

The results in Table 3 show that C16:0 and C18:0 are the main components of SFAs in polar lipids, and the proportion of C18:0 in polar lipids (approximately 7–8%) was remarkably higher than that in non-polar lipids (approximately 0.5–1%). This result indicates that most of the C18:0 binds to polar lipids. DHA and DPA are the main components of PUFAs in the polar lipids of both strains, similar to the non-polar lipids. Compared with the wild-type strain at 120 h, the proportion of SFAs in polar lipids in SR21-CCT reduced by 18.4%, and the proportions of PUFAs and DHA in polar lipids improved by 46.5% and 52.6%, respectively.
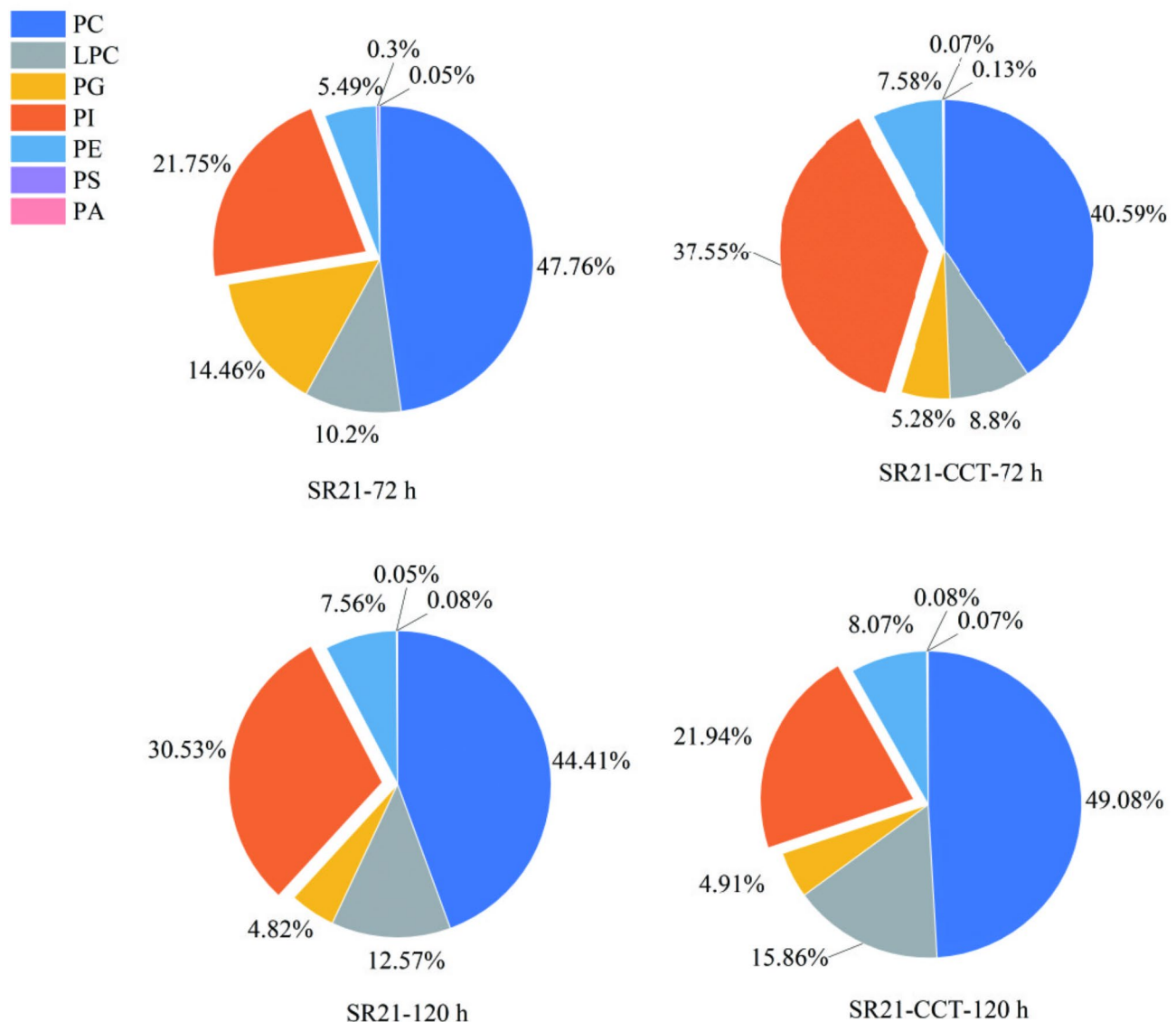
Changes of the PL profiles
The types of PLs were first tested, which consists of PC, PE, lysophosphatidylcholine (LPC), phosphatidylglycerol (PG), PI, phosphatidylserine (PS) [22], and PA (Fig. 3). The data and significance tests were shown in Table S2. PC accounted for about half of the total PLs, while the

contents of PS and PA were quite low (< 0.2%). The PL composition in SR21 and SR21-CCT at 72 and 120 h was tested to determine the effect of *CCT* overexpression on the PL synthesis pathway. As shown in Fig. 3, the percentages of PC and PI changed differently in the two strains as fermentation proceeded. The PC content of SR21 decreased from 47.8% at 72 h to 44.4% at 120 h. While in the SR21-CCT strain, the PC content increased from 40.6% at 72 h to 49.1% at 120 h. The LPC contents showed an upward change with time in both strains.

Changes in the PL contents of the different strains were then compared. At 72 h, *CCT* overexpression increased the content of PI and PE by 72.6% and 38.1%, and decreased the content of PC, PG, and LPC by 15.0%, 63.5%, and 13.7%, respectively. The percentages of PI and PG exhibited the maximum increases and decreases, respectively. In the later stage of fermentation (120 h), compared with the wild type, overexpression of *CCT* reduced the PI content by 28.1%, while enhancing the PC and LPC contents by 26.2% and 10.5%, respectively, which were completely opposite to those at 72 h. The contents of other PLs in neither strain changed significantly.

The detailed PLs species were further analyzed. A total of 33 types of PLs were detected, including 14 PC, 4 LPC, 6 PG, 4 PE, 2 PI, 2 PS, and 1 PA (Table 4). C16:0, DPA, and DHA are the major fatty acids in PLs [17]. We found

Fig. 3 Percentage of all types of phospholipids at 72 and 120 h for SR21 and SR21-CCT strains

that different phospholipids have varying preferences for esterification with fatty acids. The fatty acid side chain of PC is mainly composed of PUFAs, and the DHA proportion bound to PC exceeded half. LPC also showed an obvious preference for esterification withPUFAs, such as the DHA proportion reached 71.7% (the wild-type strain at 72 h). PG mainly binds SFAs, predominantly C16:0. The two fatty acyl chains of PI are composed of C16:0 and PUFA (C22:5 or C22:6). PE is more inclined to bind PUFAs. PS mainly binds DHA, whereas PA only binds DHA.

Figure 4A showed a heat map of each tested type of PLs based on weight data for each phospholipid in total lipids (μg/g). For the same strain at different times, except PC-C15:0/C22:6, LPC-C22:5 and LPC-C22:6, the content of the most PLs at 120 h was lower than that at 72 h,

which is due to the fact that PL synthesis mainly occurs at the early and middle stages of fermentation [23]. For a different strain at the same time, we found that the main PL species of the mutant strain were mostly more abundant than those of the wild-type strain, especially at 72 h, which was consistent with the results of Fig. 2D, that is, overexpression of *CCT* promoted the synthesis of polar lipids.

Figure 4B shows the proportions of 12 major PLs species. PC-C22:6/22:6 is the most important PC type in both strains, decreasing over time in SR21 and increasing over time in SR21-CCT. Compared to the wild-type strain, overexpression of *CCT* caused a decrease in PC-C22:6/C22:6 at 72 h and an increase at 120 h. The proportion of PC-C22:5/C22:6 in SR21-CCT exhibited changes similar to those of PC-C22:6/C22:6 compared to

Table 4 Phospholipid species in SR21 and SR21-CCT

Type	Unsaturation	Acyl composition	Content(µg/g)			
			SR21-72 h	SR21-CCT – 72 h	SR21-120 h	SR21-CCT – 120 h
PC	C30:0	C14:0/C16:0	217.4 ± 3	363.1 ± 54.8[**]	183.7 ± 73.6	287.7 ± 56.1
	C32:0	C16:0/C16:0	228.8 ± 40.9	1571 ± 255[**]	215.6 ± 27.9	446 ± 9[**]
	C36:5	C14:0/C22:5	0	144 ± 43.6[**]	98.3 ± 38.8	187 ± 20.8[*]
	C37:5	C15:0/C22:5	1046 ± 204.4	1883 ± 692.8	985.2 ± 207.3	1250 ± 97.2
	C37:6	C15:0/C22:6	6673.7 ± 527.6	6575.3 ± 846.7	5240.1 ± 1108.8	7520.8 ± 217.5[**]
	C38:5	C16:0/C22:5	4574.4 ± 1247.7	8055.4 ± 1624.7[**]	2348.7 ± 786.6	3826.3 ± 1266.6
	C38:6	C16:0/C22:6	10533.1 ± 2668.5	16262.3 ± 3120.7[*]	5168.9 ± 1472.4	8466.7 ± 721[*]
	C40:6	C18:0/C22:6	19.4 ± 4.9	244.9 ± 87.6[**]	42.5 ± 13.9	349.9 ± 14.1[**]
	C40:7	C18:1/C22:6	9 ± 0.2	146.9 ± 45.7[**]	103.2 ± 40.9	262.7 ± 14.1[**]
	C42:10	C20:4/C22:6	507.2 ± 154.2	427.1 ± 60.7	197.9 ± 27.3	901.2 ± 77.7[**]
	C42:11	C20:5/C22:6	577 ± 113.5	873.4 ± 437.5	598.1 ± 235.6	1159.6 ± 187.4
	C44:10	C22:5/C22:5	1588.4 ± 23.6	2733.2 ± 1025.3	1295.4 ± 521	1697.7 ± 386.4
	C44:11	C22:5/C22:6	10955.8 ± 428.2	15857.4 ± 2690.5	7314 ± 2443.5	9346.4 ± 675.2
	C44:12	C22:6/C22:6	18541.1 ± 3154.3	31683.8 ± 2317.8	14552.4 ± 4889.3	18433.2 ± 1706.4
LPC	C15:0	C15:0	41.6 ± 0	1650.3 ± 155	493.4 ± 264.4	1257 ± 163.4[*]
	C16:0	C16:0	113.4 ± 9	1458.6 ± 62.4[**]	83.6 ± 15.4	74.7 ± 14.6
	C22:5	C22:5	3355.4 ± 334.7	4497.8 ± 1297.7	2215.5 ± 799.4	4622.1 ± 591.8[*]
	C22:6	C22:6	8244.2 ± 1823.6	9657.7 ± 1134.4	4802.7 ± 2758.8	11424.7 ± 1112.7[*]
PG	C31:0	C15:0/C16:0	153.8 ± 30.1	148.1 ± 72.1	105 ± 43.7	257.9 ± 61.7[*]
	C32:0	C16:0/C16:0	13704.4 ± 1625	10050.9 ± 4131.6	3741.9 ± 1693	3204.4 ± 402.1
	C38:5	C16:0/C22:5	227.3 ± 53.8	381.3 ± 303.7	180.8 ± 87.3	115.1 ± 20.7
	C38:6	C16:0/C22:6	498.7 ± 48	283.9 ± 92.6	196.3 ± 90.1	361.3 ± 53.2[*]
	C44:11	C22:5/C22:6	244 ± 92.1	197 ± 45.4	190.7 ± 120	415.3 ± 84.5[*]
	C44:12	C22:6/C22:6	1319.1 ± 157.9	520.4 ± 106	492 ± 302.6	1071.7 ± 202.4[*]
PI	C38:5	C16:0/C22:5	10830.1 ± 1331.7	24204.1 ± 3615.5	11439.8 ± 5890.9	8186.9 ± 704.7
	C38:6	C16:0/C22:6	13473.5 ± 805.2	48872.2 ± 772.7	6895 ± 1403.7	15964.3 ± 147.7[**]
PE	C38:5	C16:0/C22:5	1175.1 ± 178.6	3217.4 ± 537.8[**]	1014.3 ± 499.8	1251 ± 270.4
	C38:6	C16:0/C22:6	2702.9 ± 481	6396.3 ± 1541.7[**]	2223.6 ± 899.3	2737 ± 456.7
	C44:11	C22:5/C22:6	1388.1 ± 384.2	1463.9 ± 215	563.1 ± 257.5	1412.9 ± 501.5[*]
	C44:12	C22:6/C22:6	1073.9 ± 345.2	3864.6 ± 330.3[**]	1314.1 ± 731.5	3547.3 ± 799.3[*]
PS	C28:0	C14:0/C14:0	63.9 ± 24.7	52.2 ± 38	27 ± 7.8	26.8 ± 6.6
	C44:12	C22:6/C22:6	266.5 ± 24.3	86.8 ± 7.9[**]	14.2 ± 4.8	56.5 ± 6.5[**]
PA	C44:12	C22:6/C22:6	59.9 ± 3.7	250.1 ± 70.2[**]	63.9 ± 6.1	81.8 ± 12.4[*]

Note: *p-value < 0.05 and **p-value < 0.01, compared to SR21 at each time
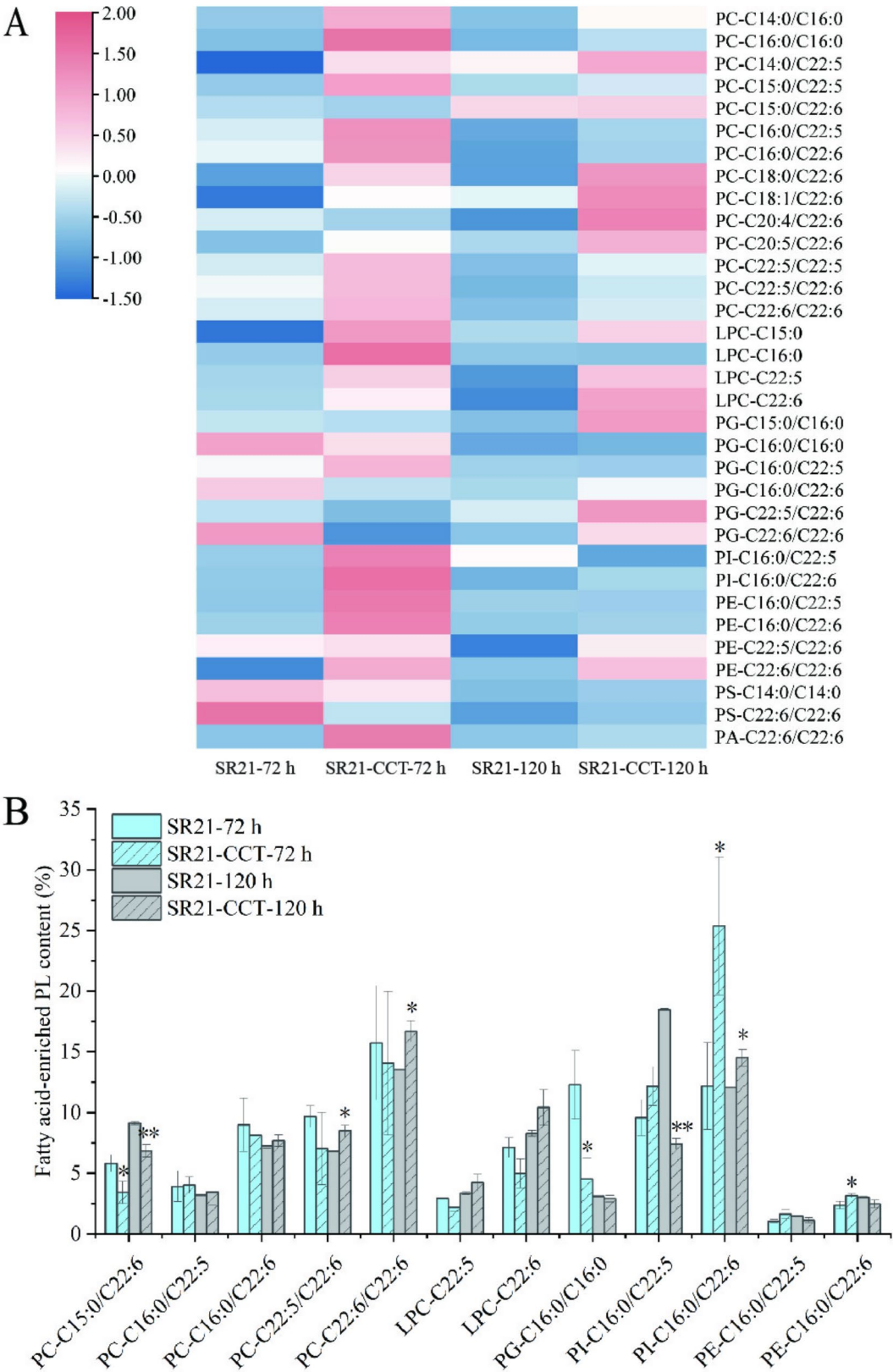
SR21. LPC-C22:5 and LPC-C22:6, the two main species of LPC, increased with time in both strains, the content of which was increased in the *CCT*-overexpression strain. As the main type of PG, the PG-16:0/16:0 proportion sharply declined at 72 h in SR21-CCT compared to that in the control strain, while it showed the same value at 120 h. Interestingly, the content of PI-C16:0/C22:6 in the wild-type strain showed no difference at 72 and 120 h; however, the content was significantly enhanced at 72 h in SR21-CCT, which was twice that of the wild-type strain, after it dropped by 42.7% at 120 h, which was only slightly higher than that of the wild-type strain. The two main types of PE showed similar changes in the two strains, the content of which at 72 h in SR21-CCT was slightly higher than that in SR21, but slightly lower than that in SR21 at 120 h. In summary, the proportions of PLs, including PC, LPC, PG, and PI, changed in the mutant strain. Among

them, the content of DHA- esterified PLs in the SR21-CCT strain increased significantly, while that of C16:0-esterified PLs significantly decreased. This result verified that overexpression of *CCT* can remarkably improve the accumulation of PUFAs, especially DHA, and reduce the synthesis of SFAs (C16:0-based).
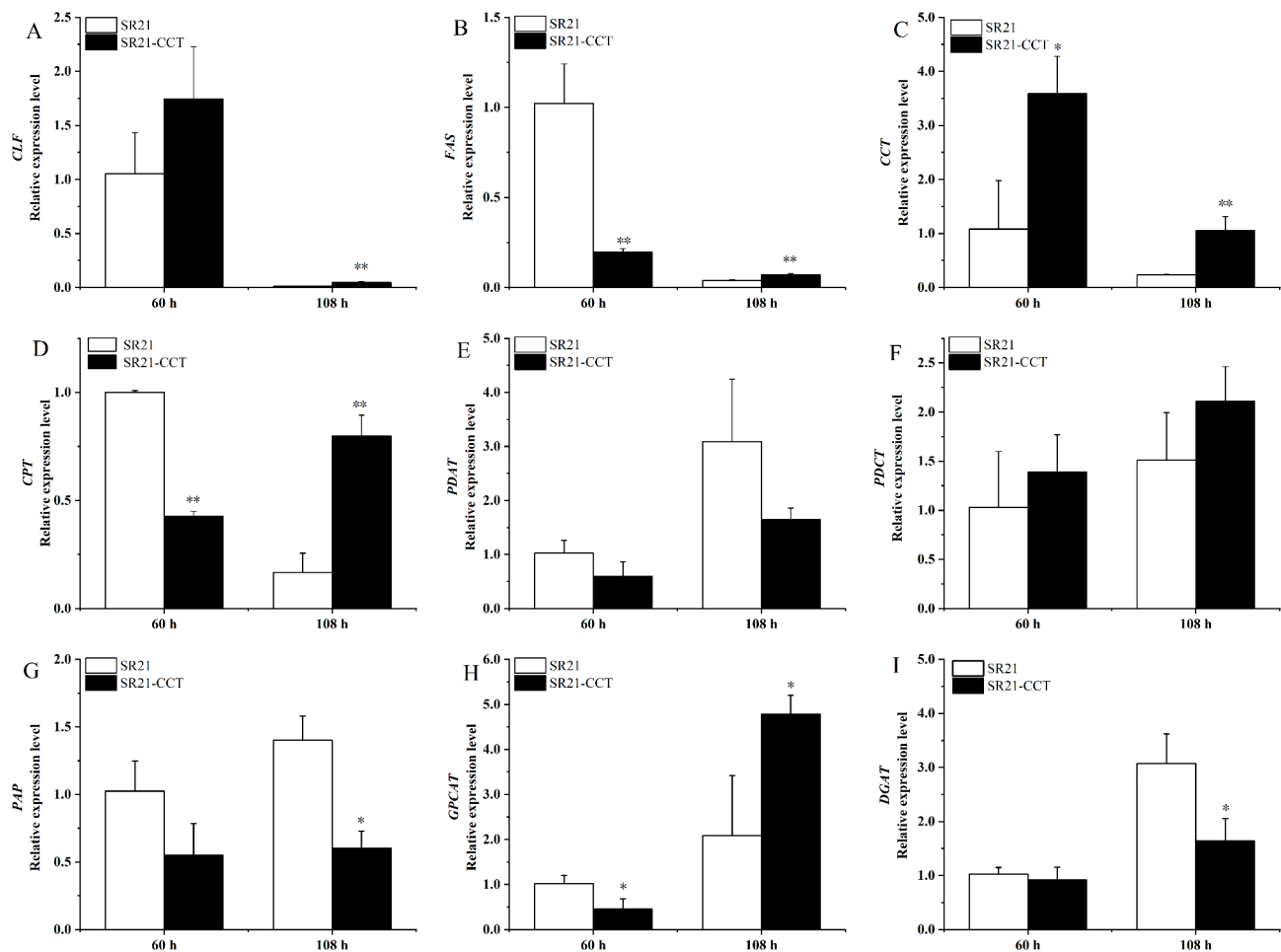
Effects of *CCT* overexpression on the transcriptional levels of key genes in lipid metabolism pathway

In *Schizochytrium*, there are two pathways for synthesizing fatty acids——anaerobic PKS pathway (PUFA) and aerobic FAS pathway (SFA) [24, 25]. The chain length factor (*CLF*) gene and fatty acid synthase (*FAS*) gene are the key genes for these two pathways respectively [7, 26, 27]. As shown in Fig. 5A and B, *CLF* and *FAS* exhibited different behaviors after overexpression of *CCT*. At 60 h, compared with the control, the transcription level of *CLF*

Fig. 4 The heat map of phospholipid content Z-scores (**A**) and proportion of major phospholipids **(B) in wild-type and SR21-CCT strains.** Note: *p-value < 0.05 and **p-value < 0.01, compared to SR21 at each time

Fig. 5 The transcript level of key genes in wild-type strain and SR21-CCT strain: *CLF* (**A**); *FAS* (**B**); *CCT* (**C**); *CPT* (**D**); *PDAT* (**E**); *PDCT* (**F**); *PAP* (**G**); *GPCAT* (**H**); *DGAT*(I). Note: **p*-value < 0.05 and ***p*-value < 0.01, compared to SR21 at each time

in the mutant strain increased by about 40% whereas that of *FAS* underwent a substantial decrease of about 80% in SR21-CCT; at 108 h, overexpression of *CCT* slightly increased the transcript levels of *CLF* and *FAS*. CCT and CPT are two key enzymes that synthesize PC via *de novo* pathway [28, 29]. As shown in Fig. 5C, the expression level of *CCT* in both strains at 60 h was higher than that at 108 h, indicating that PC synthesis is more active in the early fermentation stage. The transcription level of *CCT* in the mutant strain was higher than that in the control strain, indicating that *CCT* overexpression is favorable for the PC synthesis pathway. CPT is responsible for using CDP-cho and DAG to form PC. Compared to the wild-type strain, overexpression of *CCT* inhibited the expression level of *CPT* at the early stage but facilitated it at the late stage (Fig. 5D). This may be related to the regulated DAG synthesis derived from the reduced *FAS* expression at 60 h and enhanced expression at 108 h.

PC: DAG choline phosphotransferase (PDCT) mediates the conversion of PC to DAG, then DAG is converted to TAG under the action of diacylglycerol acyltransferase

(DGAT) [30]. Phospholipid: DAG acyltransferase (PDAT) catalyzes the direct transfer of acyl groups from the *sn*-2 position of PLs to DAG to form TAG in plant [31]. Compared with the wild-type strain, the transcription level of *PDCT* was not obviously increased at both 60 and 108 h after overexpression of *CCT* (Fig. 5E), while the transcription level of PDAT was decreased two-fold after overexpression of *CCT* (Fig. 5F), speculating that overexpression of *CCT* in *Schizochytrium* may reduce the direct synthesis pathway of TAG from PC and enhanced the DAG pool converted from PC to TAG [32]. Phosphatidic acid phosphatase (PAP) catalyzes DAG synthesis from PA via the Kennedy pathway, and then DAG is further converted into TAG under the action of diacylglycerol acyltransferase (DGAT) [33]. The transcription level of *PAP* and *DGAT* in SR21-CCT strain decreased about 50% (Fig. 5G) compared to that in SR21, indicating that the synthesis of TAG by PA was weakened. GPCAT is a key enzyme in the GPC acylation pathway that synthesizes LPC, which can accept one fatty acid chain to form PC. Figure 5H showed a slight decrease in *GPCAT*

transcription levels at 60 h but a significant increase at 108 h after overexpression of *CCT*, which enhanced LPC at the late stage of fermentation and the corresponding increase in PC synthesis at 120 h (Fig. 3).

Discussion

Plant and algal studies have identified a close association between the PL pathway and glyceride synthesis [34–36], particularly in the accumulation of unsaturated fatty acids in glycerides. Lipid droplets form the main lipid store in eukaryotic cells and are covered by protein-containing PL monolayers [37, 38]. The synthesis and accumulation of TLs are closely related to those of PLs. Researchers have not yet clearly explored the mechanisms of conversion between PL synthesis, TAG production, and PUFA accumulation in *Schizochytrium*.

Lipid composition analysis (Fig. 2D) shows that PL synthesis in *Schizochytrium* is active at the early stage of cell growth (48 h), before gradually declining at the middle stage (from 72 to 96 h), and remaining at a low level in the later period (after 96 h). DHA production corresponds to a slow and remarkable increase at the early and middle stages and a stable level after 96 h (Fig. 2B). The overexpression of *CCT* promoted PL synthesis during the whole process, especially in the early stages, resulting in the final enhancement of TLs production and DHA accumulation (Fig. 2B), indicating that PL metabolism is closely related to DHA accumulation. In addition, the transcription level of *FAS* decreases significantly in the early stage of fermentation, whereas that of *CLF* increases, thereby resulting in a significant decrease in the SFA proportion and increase in the PUFA proportion (Table 1), promoting DHA synthesis in *Schizochytrium*, demonstrating that strengthening the pathway of PC synthesis contributes to PUFAs and DHA accumulation.

The proportion of DHA in non-polar lipids continues to increase (Table 2), whereas that in polar lipids shows a clear increase from 48 to 72 h, before decreasing continuously. This is consistent with the migration of DHA from polar lipids to TAG for storage, as proposed in other studies [10]. The overexpression of *CCT* enhanced the DHA proportion in both polar and non-polar lipids, increasing by 51.5% and 52.6% at 120 h compared with that in the wild-type strain, respectively, indicating that *CCT* overexpression may promote the final DHA accumulation in TLs by strengthening PL synthesis to improve the esterification rate of DHAin PLs, rather than increasing the migration rate of DHA from PLs to TAG.
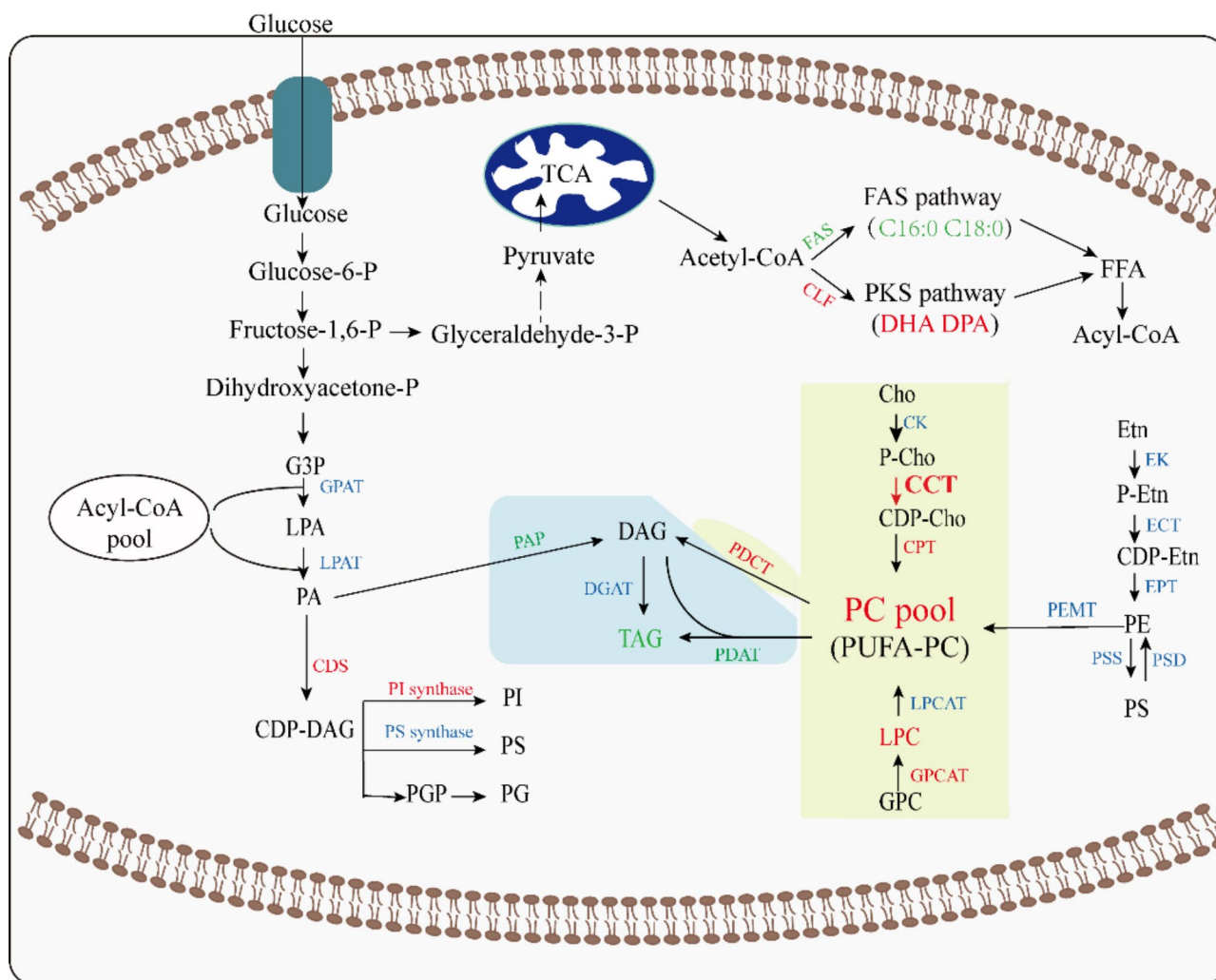
As the key enzyme in the *de novo* PC synthesis pathway, *CCT* overexpression changed the PL composition (Fig. 3). PC is the main PL type, the synthesis of which is positively correlated with the accumulation of DHA, owing to its predominant DHA esterification (Table 4; Fig. 4). Compared to the wild-type, the PC content in

SR21-CCT increases at 120 h (Fig. 3), and the expression of *CPT* and *CCT* genes (Fig. 5C and D) in SR21-CCT significantly improves at 108 h, indicating that the *de novo* pathway of PC biosynthesis was promoted. LPC content (Fig. 3) and *GPCAT* expression (Fig. 5H) in SR21-CCT also exhibited an increase at 120 h compared to the wild-type strain, indicating that the GPC acylation pathway was also strengthened, which is conducive to the esterification of more released non-esterified DHA to LPC and the transfer of DHA to PC to form DHA-PC, resulting in the enhancement of its content (Fig. 4). Glab found that the loss of GPCAT led to a decrease in the PC content [18]. Therefore, the acylation of GPC is important for maintaining PC levels.

In eukaryotes, PC can be transformed into TAG via two steps of PDCT and DGAT catalysis [39] or by a single step of PDAT catalysis [40]. Many studies have shown that plants usually use PC-derived DAG to synthesize PUFA-containing TAGs, and PDCT-mediated transformation provides approximately 66% of PUFAs from PC to TAG flux [41]. The increased transcription of *PDCT* and decreased transcription of *PDAT* in the mutant strain imply the *CCT* overexpression could accelerate the conversion of PC to TAG via the PDCT catalytic pathway. Accordingly, TAG synthesis via the Kennedy pathway was markedly inhibited as reflected by the down-regulated expression of PAP (Fig. 5G).

PI is an important signaling molecule that regulates cell signal transduction and metabolic processes, especially lipid metabolism, and binds equally to PUFAs and SFAs (Table 4). After entering the lipid transformation period (120 h), the cells require more PI for signal transduction and metabolic regulation. The DHA accumulation in the mutant strain at 72 h and 120 h was associated with the increase of PI-C16:0/C22:6 and PC-C22:6/C22:6, respectively. In addition, the percentage of PG in the mutant strain decreased substantially at 72 h, whereas it was close to that in the wild-type strain at 120 h. Previous studies have shown that the biological function of PG is closely linked to cell growth and that cell division is impeded when PG is deficient [42]. PG species mainly incorporating 16:0 most efficiently complemented cell growth [43]. PG-C16:0/16:0 is the most important type of PG, and changes in its levels in SR21-CCT correspond to cell growth; that is, decreased PG levels result in lower cell growth (Fig. 2A and 3).

In summary, *CCT* overexpression could significantly increase lipid synthesis, particularly promoting DHA accumulation. As shown in Fig. 6, we hypothesized that *CCT* overexpression in *Schizochytrium* attenuates the Kennedy pathway of TAG synthesis and enhances the PC synthesis pathway to strengthen the esterification of DHA to PC, which then migrates from PC to TAG for

Fig. 6 Metabolic mechanism of overexpressing *CCT* in *S. limacinum* SR21. The upward genes or products were shown in red font; the downward changes were indicated in green font

storage, thereby promoting the final accumulation of DHA in TAGs.

Conclusion

In the present study, we investigated the role of *CCT* in lipid metabolism in *Schizochytrium* for the first time. Overexpression of *CCT* exerted a profound effect on TL production by enhancing PL synthesis. The increased synthesis of PC caused more non-esterified DHA to esterified to PC. The bound DHA was subsequently transferred to DAG to form DHA-TAG. Enhancement of PL synthesis decreased SFA accumulation in TAG via the Kennedy pathway, resulting in increased PUFA accumulation in TAG through the PC pathway in the mutant strain. Collectively, cellular metabolism and lipid synthesis can be regulated by modulating the PL pathway, thereby mediating DHA production in *Schizochytrium*. This study provides new insights into the transformation of PLs and DHA-TAG synthesis.

Abbreviations

CCT	Phosphocholine cytidylyltransferase
CK	choline kinase
CLF	chain length factor
CPT	choline phosphotransferase
DAG	diacylglycerol
DCW	dry cell weight
DGAT	diacylglycerol acyltransferase
DHA	docosahexaenoic acid
DHA-FFA	free fatty acid DHA
DPA	docosapentaenoic acid
EPA	eicosapentaenoic acid
FAMEs	fatty acid methyl ester
FAS	fatty acid synthase
GC	gas chromatography
GPC	glycerophosphorylcholine
GPCAT	glycerophosphorylcholine acyltransferase
LPC	lysophosphatidylcholine
LPCAT	lysophosphatidylcholine acyltransferase
PA	phosphatidic acid
PC	phosphatidylcholine
PCho	phosphocholine
PDAT	Phospholipid: DAG acyltransferase
PDCT	PC:DAG choline phosphotransferase
PE	phosphatidylethanolamine

PG   phosphatidylglycerol
PI   phosphatidylinositol
PKS   polyketide synthase
PLs   phospholipids
PS   phosphatidylserine
PUFA   polyunsaturated fatty acid
SFA   saturated fatty acid
TAG   triacylglycerol
TLC   Thin-layer chromatography
TLs   Total lipids

Supplementary Information

The online version contains supplementary material available at https://doi.or g/10.1186/s12934-025-02703-2.

Supplementary Material 1

Data availability
The sequence data generated for this study can be accessed via GenBank: htt ps://www.ncbi.nlm.nih.gov/genbank/

Declarations

Ethics approval and consent to participate
Not applicable.

Consent for publication
Not applicable.

Competing interests
The authors declare no competing interests.

References
1. Ye C, Qiao W, Yu X, Ji X, Huang H, Collier JL, Liu L. Reconstruction and analysis of the genome-scale metabolic model of schizochytrium limacinum SR21 for docosahexaenoic acid production. BMC Genomics. 2015;16:799.
2. Ling X, Guo J, Liu X, Zhang X, Wang N, Lu Y, Ng IS. Impact of carbon and nitrogen feeding strategy on high production of biomass and docosahexaenoic acid (DHA) by schizochytrium Sp. LU310. Bioresour Technol. 2015;184:139–47.
3. Du F, Wang YZ, Xu YS, Shi TQ, Liu WZ, Sun XM, Huang H. Biotechnological production of lipid and terpenoid from thraustochytrids. Biotechnol Adv. 2021;48:107725.
4. Yang Q, Xie Z, Zheng X, Li K, Lu T, Lu Y, Chen C, Ling X. Genetic regulation and fermentation strategy for squalene production in schizochytrium Sp. Appl Microbiol Biotechnol. 2022;106:2415–31.
5. Tang X, Man Y, Hu X, Xu X, Ren L. Identification of carotenoids biosynthesis pathway in schizochytrium Sp. and utilization in Astaxanthin biosynthesis. Enzyme Microb Technol. 2022;156:110018.
6. Lawson LD, Hughes BG. Human absorption of fish oil fatty acids as triacylglycerols, free acids, or Ethyl esters. Biochem Biophys Res Commun. 1988;152:328–35.
7. Chi G, Xu Y, Cao X, Li Z, Cao M, Chisti Y, He N. Production of polyunsaturated fatty acids by schizochytrium (Aurantiochytrium) spp. Biotechnol Adv. 2022;55:107897.
8. Zhao XM, Qiu X. Very long chain polyunsaturated fatty acids accumulated in triacylglycerol are channeled from phosphatidylcholine in *Thraustochytrium*. Front Microbiol 2019, 10.
9. Zhao X, Qiu X. Analysis of the biosynthetic process of fatty acids in *Thraustochytrium*. Biochimie. 2018;144:108–14.
10. Yue XH, Chen WC, Wang ZM, Liu PY, Li XY, Lin CB, Lu SH, Huang FH, Wan X. Lipid distribution pattern and transcriptomic insights revealed the potential mechanism of docosahexaenoic acid traffics in schizochytrium Sp. A-2. J Agric Food Chem. 2019;67:9683–93.
11. Nutahara E, Abe E, Uno S, Ishibashi Y, Watanabe T, Hayashi M, Okino N, Ito M. The glycerol-3-phosphate acyltransferase PLAT2 functions in the generation of DHA-rich glycerolipids in aurantiochytrium limacinum F26-b. PLoS ONE. 2019;14:e0211164.
12. Zhang Y, Cui X, Lin S, Lu T, Li H, Lu Y, Cao M, Lin X, Ling X. Knockout of a PLD gene in schizochytrium limacinum SR21 enhances docosahexaenoic acid accumulation by modulation of the phospholipid profile. Biotechnol Biofuels Bioprod. 2024;17:16.
13. Kennedy EP, Weiss SB. The function of cytidine coenzymes in the biosynthesis of phospholipides. J Biol Chem. 1956;222:193–214.
14. Gibellini F, Smith TK. The Kennedy pathway–De Novo synthesis of phosphatidylethanolamine and phosphatidylcholine. IUBMB Life. 2010;62:414–28.
15. Munoz CF, Sudfeld C, Naduthodi MIS, Weusthuis RA, Barbosa MJ, Wijffels RH, D'Adamo S. Genetic engineering of microalgae for enhanced lipid production. Biotechnol Adv. 2021;52:107836.
16. Zhang Y, Wu G, Zhang Y, Wang X, Jin Q, Zhang H. Advances in exogenous docosahexaenoic acid-containing phospholipids: sources, positional isomerism, biological activities, and advantages. Compr Rev Food Sci Food Saf. 2020;19:1420–48.
17. Li LL, Chang M, Tao GJ, Wang XS, Liu Y, Liu RJ, Jin QZ, Wang XG. Analysis of phospholipids in schizochytrium Sp. S31 by using UPLC-Q-TOF-MS. Anal Methods. 2016;8:763–70.
18. Glab B, Beganovic M, Anaokar S, Hao MS, Rasmusson AG, Patton-Vogt J, Banas A, Stymne S, Lager I. Cloning of Glycerophosphocholine acyltransferase (GPCAT) from fungi and plants. J Biol Chem. 2016;291:25066–76.
19. King WR, Singer J, Warman M, Wilson D, Hube B, Lager I, Patton-Vogt J. The Glycerophosphocholine acyltransferase Gpc1 contributes to phosphatidylcholine biosynthesis, long-term viability, and embedded hyphal growth in Candida albicans. J Biol Chem. 2024;300:105543.
20. Pricejones MJ, Harwood JL. The control of Ctp - Choline-Phosphate cytidylyltransferase activity in pea (Pisum-Sativum-L). Biochem J. 1986;240:837–42.
21. Ling X, Zhou H, Yang Q, Yu S, Li J, Li Z, He N, Chen C, Lu Y. Functions of Enyolreductase (ER) Domains of PKS Cluster in Lipid Synthesis and Enhancement of PUFAs Accumulation in Schizochytrium limacinum SR21 Using Triclosan as a Regulator of ER. *Microorganisms* 2020, 8.
22. de Marco Castro E, Kampschulte N, Murphy CH, Schebb NH, Roche HM. Oxylipin status, before and after LC n-3 PUFA supplementation, has little relationship with skeletal muscle biology in older adults at risk of sarcopenia. Prostaglandins Leukot Essent Fat Acids. 2023;189:102531–102531.
23. Morita E, Kumon Y, Nakahara T, Kagiwada S, Noguchi T. Docosahexaenoic acid production and lipid-body formation in schizochytrium limacinum SR21. Mar Biotechnol (NY). 2006;8:319–27.
24. Metz JG, Kuner J, Rosenzweig B, Lippmeier JC, Roessler P, Zirkle R. Biochemical characterization of polyunsaturated fatty acid synthesis in schizochytrium: release of the products as free fatty acids. Plant Physiol Biochem. 2009;47:472–8.
25. Metz JG, Roessler P, Facciotti D, Levering C, Dittrich F, Lassner M, Valentine R, Lardizabal K, Domergue F, Yamada A, et al. Production of polyunsaturated fatty acids by polyketide synthases in both prokaryotes and eukaryotes. Science. 2001;293:290–3.
26. Tang Y, Tsai SC, Khosla C. Polyketide chain length control by chain length factor. J Am Chem Soc. 2003;125:12708–9.

27. Santin O, Yuet K, Khosla C, Moncalian G. Structure and mechanism of the Ketosynthase-Chain length factor Didomain from a prototypical polyunsaturated fatty acid synthase. Biochemistry. 2020;59:4735–43.

28. Horibata Y, Sugimoto H. Differential contributions of choline phosphotransferases CPT1 and CEPT1 to the biosynthesis of choline phospholipids. J Lipid Res 2021, 62.

29. Sato N, Mori N, Hirashima T, Moriyama T. Diverse pathways of phosphatidylcholine biosynthesis in algae as estimated by labeling studies and genomic sequence analysis. Plant J. 2016;87:281–92.

30. Lu CF, Xin ZG, Ren ZH, Miquel M, Browse J. An enzyme regulating triacylglycerol composition is encoded by the ROD1 gene of Arabidopsis. Proc Natl Acad Sci USA. 2009;106:18837–42.

31. Dahlqvist A, Stahl U, Lenman M, Banas A, Lee M, Sandager L, Ronne H, Stymne S. Phospholipid:diacylglycerol acyltransferase: an enzyme that catalyzes the acyl-CoA-independent formation of triacylglycerol in yeast and plants. Proc Natl Acad Sci U S A. 2000;97:6487–92.

32. Hu ZH, Ren ZH, Lu CF. The phosphatidylcholine Diacylglycerol cholinephosphotransferase is required for efficient hydroxy fatty acid accumulation in Transgenic Arabidopsis. Plant Physiol. 2012;158:1944–54.

33. Jin HH, Jiang JG. Phosphatidic acid phosphatase and Diacylglycerol acyltransferase: potential targets for metabolic engineering of microorganism oil. J Agric Food Chem. 2015;63:3067–77.

34. Ogasawara Y, Cheng JL, Tatematsu T, Uchida M, Murase O, Yoshikawa S, Ohsaki Y, Fujimoto T. Long-term autophagy is sustained by activation of CCTβ3 on lipid droplets. Nat Commun 2020, 11.

35. Xiao Q, Pan X, Xu Y, Singer SD, Chen GQ. Genome-wide characterization of plant CTP:phosphocholine cytidylyltransferases through evolutionary, biochemical, and structural analyses. Plant J. 2023;115:833–45.

36. Izrael R, Marton L, Nagy GN, Palinkas HL, Kucsma N, Vertessy BG. Identification of a nuclear localization signal in the plasmodium falciparum CTP: phosphocholine cytidylyltransferase enzyme. Sci Rep. 2020;10:19739.

37. Chorlay A, Monticelli L, Verissimo Ferreira J, Ben M, Ajjaji K, Wang D, Johnson S, Beck E, Omrane R, Beller M. Membrane asymmetry imposes directionality on lipid droplet emergence from the ER. Dev Cell. 2019;50:25–e4227.

38. Cornell RB. Membrane lipids assist catalysis by CTP: phosphocholine cytidylyltransferase. J Mol Biol. 2020;432:5023–42.

39. Bates PD, Browse J. The significance of different Diacylglycerol synthesis pathways on plant oil composition and bioengineering. Front Plant Sci. 2012;3:147.

40. Fattore N, Bucci F, Bellan A, Bossi S, Maffei ME, Morosinotto T. An increase in the membrane lipids recycling by PDAT overexpression stimulates the accumulation of triacylglycerol in Nannochloropsis Gaditana. J Biotechnol. 2022;357:28–37.

41. Bates PD, Fatihi A, Snapp AR, Carlsson AS, Browse J, Lu CF. Acyl editing and headgroup exchange are the major mechanisms that direct polyunsaturated fatty acid flux into triacylglycerols. Plant Physiol. 2012;160:1530–9.

42. Kóbori TO, Uzumaki T, Kis M, Kovács L, Domonkos I, Itoh S, Krynická V, Kuppusamy SG, Zakar T, Dean J, et al. Phosphatidylglycerol is implicated in divisome formation and metabolic processes of cyanobacteria. J Plant Physiol. 2018;223:96–104.

43. Endo K, Abe M, Kawanishi N, Jimbo H, Kobayashi K, Suzuki T, Nagata N, Miyoshi H, Wada H. Crucial importance of length of fatty-acyl chains bound to the sn-2 position of phosphatidylglycerol for growth and photosynthesis of synechocystis Sp. PCC 6803. Biochim Et Biophys Acta-Molecular Cell Biology Lipids 2022, 1867.

Publisher's note